THE UNIVERSITY OF MICHIGAN
INDUSTRY PROGRAM OF THE COLLEGE OF ENGINEERING

AN APPLICATION OF A GAS TURBINE ENGINE PERFORMANCE COMPUTER TO A TWIN-SPOOL ENGINE

W. L. Larrowe
M. M. Spencer
S. R. Lampert

This is a Report of Project Work Done
by the Engineering Research Institute

November, 1957

IP-250

TABLE OF CONTENTS

LIST OF FIGURES

SYMBOLS

Symbol	Definition
$[X]$	$\log_{10} X$
h	Absolute enthalpy (Btu/lb)*
h_s	Sea level standard enthalpy (123.96 Btu/lb)
T	Total temperature (degrees Rankine)*
T_s	Sea level standard temperature (518.4° R)
J	Mechanical equivalent of heat (778 ft-lb/Btu)
P	Total absolute pressure (psia)*
P_s	Standard pressure at sea level (14.7 psia)
N_L	Low-pressure compressor rotor speed (revolutions per minute)
N_H	High-pressure compressor rotor speed (revolutions per minute)
θ	Referred temperature $\left(\frac{T}{T_s}\right)^*$
ϕ	Referred enthalpy $\left(\frac{h}{h_s}\right)^*$
δ	Referred total pressure $\left(\frac{P}{P_s}\right)^*$
I	Rotor moment of inertia (slug-ft^2)
ω	Angular velocity (radians per second)
W	Gas flow rate (lbs/second)*
W_f	Fuel flow rate (lbs/second)
W_{BL}	Bleed air flow rate (lbs/second)
M_N	Mach number
A_j, A_T	Exhaust nozzle area (sq ft)
η	Efficiency
F_g	Gross thrust

*Numerical subscripts refer to stations in the engine, as defined by Figure 1.

ABSTRACT

The gas turbine engine performance computer as described in Wright Air Development Center Technical Report 54-577, Parts I and II, has been extended in capability to represent a twin-spool engine. A year of successful operation with this version of the computer has resulted in improvements in computer techniques, improvements in methods for preparing and using function generators of two variables, and development of various new ways of obtaining engine data.

FOREWORD

This report describes technical progress in the method of using an analog computer for obtaining the static and dynamic performance of gas turbine engines as described in two previous reports (WADC TR 54-577, Parts I and II). The more recent work was performed under two consecutive projects; the first was sponsored by Westinghouse Electric Corporation, Aviation Gas Turbine Division, Kansas City, Missouri, and the second by Allison Division of General Motors Corporation, Indianapolis, Indiana.

INTRODUCTION

During the fall of 1953, the Air Force sponsored a research project at The University of Michigan Willow Run Research Center (now Willow Run Laboratories) to determine the feasibility of a proposed method of computing the dynamic and steady-state performance of a gas-turbine engine. The method required the use of standard, commercially available, analog computing equipment, but it differed from conventional analog methods in two respects. First, it required the use of a number of special electro-mechanical "map-readers," and second, it involved representing variables by d-c analog voltages which were proportional to the logarithms of these variables instead of being proportional to the values of the variables themselves. The computing method is described in the final report for this first project. This report was published by The University of Michigan, Engineering Research Institute as UMM-143 and by the Air Force as WADC TR 54-577, Part I.

Since time had permitted only a brief investigation of the computing techniques as applied to a simple unaugmented turbojet engine, and since the method showed considerable promise, the Air Force contract was extended for a year to permit development and testing of methods of applying the techniques to more complex engine configurations and to arrange for the computer to be demonstrated to representatives from various fields of industry associated with gas-turbine engines and their controls. The results of the second phase of this project are given in WADC TR 54-577, Part II (also published by The University of Michigan as 2149-1-F).

Since the termination of the Air Force contract, the computing method has been applied at the Willow Run Laboratories to two different engines, and a number of improvements have been added. This report is intended as a supplement to the two reports already published and thus does not describe the simulation method in detail. Instead, it describes the various improvements of arranging and scaling the computer diagram (road map) and deals with methods of operating the computer to obtain desired information about the engine. The report also briefly describes the application of the computing method to a twin-spool turbojet engine and gives a method of checking simulated engine control circuits for correct operation.

The results of improvements in techniques of scaling and operating are illustrated by the fact that the latest engine (a twin-spool turbojet engine with a number of refinements) was operated successfully with twelve map readers and twenty single-variable function generators.

I

ANALOG PERFORMANCE-COMPUTATION FOR TWIN-SPOOL TURBOJET ENGINE

1.1 Description of Twin-Spool Engine

During 1956, the gas turbine engine performance computer was used to compute the dynamic and static performance of a twin-spool turbojet engine. A simplified diagram of such an engine is shown in Figure 1. This engine has two compressors, a combustor, two turbines, and an exhaust nozzle. The inner compressor and the inner turbine are joined by a hollow drive shaft. This assembly makes up the high-pressure rotor. The outer, or low-pressure compressor is connected to the outer turbine by a solid shaft, passing through the hollow shaft of of the high-pressure rotor. This assembly of the outer turbine and outer compressor is called the low-pressure rotor. Air entering the engine is compressed by the low-pressure compressor and then by the high-pressure compressor. The air from the high-pressure compressor is then mixed with fuel and burned in the combustor. The hot gases exit through the high-pressure and low-pressure turbines, imparting energy to these devices to drive the corresponding rotors, and finally pass through the exhaust nozzle. Various arrangements for bleeding and by-passing air are often used in order to avoid compressor surge and to obtain better engine performance, but these are not shown in Figure 1 since they are not necessary for the explanations which follow in this report.

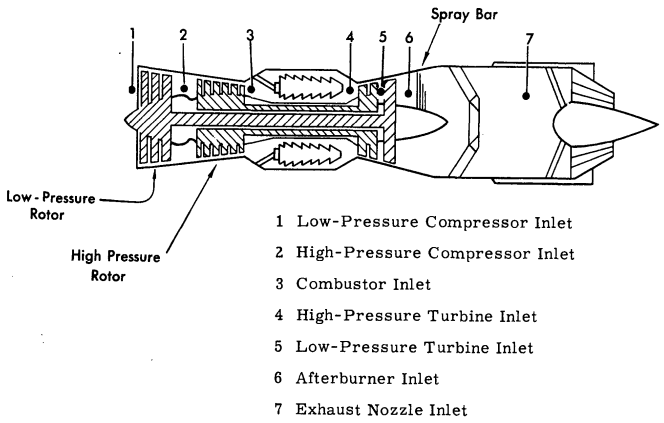

FIG. 1 STATIONS OF A TWIN-SPOOL TURBOJET ENGINE

1.2 Information Flow in a Twin-Spool-Engine Performance Computer

A block diagram showing information flow in the performance computer for the twin-spool engine is shown in Figure 2. Pressure information originates at the exhaust nozzle and flows "upstream," while temperature and air flow rate information originate at the compressor and flow "downstream." Note that pressures are used in referred form (ratio of the pressure to standard atmospheric pressure at sea level) or δ's, and that enthalpies are used instead of temperatures. Plotting the compressor and turbine characteristics using enthalpy instead of temperature removes any difficulties encountered with variable specific heats. The general circuitry for the computer for the double compressor is presented on page 57 of Reference 1, and the circuitry and description of the dual turbine are given on page 59 of Reference 2. These diagrams use temperatures instead of enthalpies, but since the conversion to use enthalpies is simple and straightforward, it will not be discussed here.

The functional relations shown in each block, except the combustor, are those which require the use of function generators of two variables, or electronic map readers. Other functional relations, giving change in air-weight flow due to bleeding air or by-passing air, are not shown. In previous work with single spool engines, the operation of the exhaust nozzle was described by two functions of single variables, one given corrected air weight flow as a function of nozzle pressure ratio, and the other given corrected thrust as a function of nozzle pressure ratio. These curves were used with the assumptions that the nozzle discharge coefficient, C_D, and the nozzle velocity coefficient, C_V, were essentially constant over the expected range of operation.

As shown in Figure 2, the performance computer for the twin-spool engine represented the exhaust nozzle in a more refined manner. The nozzle discharge coefficient, C_D, was generated as a function of both nozzle area and nozzle pressure ratio. The corrected air-weight flow through the nozzle and the corrected thrust were each specified as functions of the enthalpy of the nozzle inlet air, as well as the nozzle pressure ratio. Thus, the nozzle computer for the twin-spool engine required a total of three dual-input map readers.

The computer arrangement represented by the block diagram in Figure 2 was found to operate quite satisfactorily, and large amounts of data were obtained from it, both transient and steady-state.

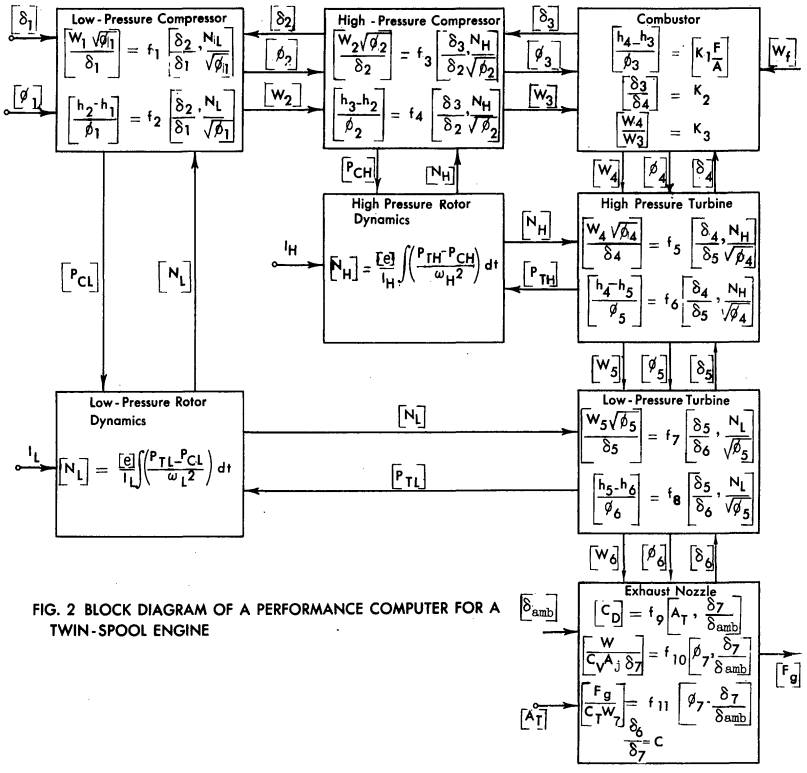

FIG. 2 BLOCK DIAGRAM OF A PERFORMANCE COMPUTER FOR A TWIN-SPOOL ENGINE

2

NEW PERFORMANCE-COMPUTER TECHNIQUES

2.1 Use of Enthalpy Instead of Temperature

The earlier versions of the gas turbine engine performance computer used temperatures and temperature changes as variables throughout the engine. In order to convert the temperature rises in the compressors and temperature drops in the turbine into corresponding energy changes, it was necessary to multiply by the appropriate specific heats of the gas. Since the values of specific heat depend upon the temperature, either a variable specific heat had to be used, thus increasing the complexity of the computer, or the average values of specific heat had to be used, thus increasing the error.

For the most recent engine, it was decided to use enthalpy rather than temperature as the basic variable. Thus, the compressor maps were plotted to give corrected enthalpy rise instead of corrected temperature rise. The resulting computer circuit gave the accuracy obtainable with variable specific heats, while retaining the simplification obtainable with constant specific heats. In the turbines, however, the air velocity was quite high, and engineers from the engine manufacturer felt that the use of enthalpy as a parameter in the various corrected variables plotted on the turbine maps would lead to significant errors. In these maps, therefore, a quantity, $\theta^{\star}$, corresponding to referred static temperature was used instead of ϕ, the referred enthalpy. Later, it was discovered that this correction made no appreciable difference in the results, since the curve relating $\theta^{\star}$ and ϕ was almost a straight line. With higher air velocities in the turbines, however, the difference would have been greater.

2.2 Soldering With Indium

Each silver line on the surface of a function-generating plate for a map reader must be driven at an an appropriate analog voltage. This means, of course, that each line must be connected through a separate wire to a potentiometer arm or some other voltage source. Previously, these voltage-feed wires were attached to the function generating plates for the map readers by soldering their ends to small tabs made of brass shim-stock and cementing the tabs to the desired spot on the plate with silver paint, as described in Reference 3. Recently, however, the wires have been soldered directly to the glass, using the metal indium as a solder. A small soldering iron is used to tin the surface of the glass quite readily with indium, and the bare wire is soldered directly to the tinned surface, using more indium. No flux of any kind is needed.

Wires may be fastened much more permanently in this manner, and they may be removed easily by unsoldering them. After the wire has been soldered into place on the glass, the silver line to which the wire is to be connected is extended to the soldered spot by using more silver paint.

2.3 Change of Surge-Line Presentation on Compressor Maps

In the earlier versions of the gas turbine engine performance computer, the surge line on the compressor maps was marked, and the conducting material was removed along its length. This was done to prevent "fringing" effects due to the adjacent surge region where there were no lines. A part of a map of this type is illustrated in Figure 3a. Because of the curving of the conducting lines on the maps, the electrical interpolation of the compressor characteristics along the surge line was found to be quite poor. This was remedied by extending each conducting line a short distance into the surge region and marking the surge line with quarter-inch black

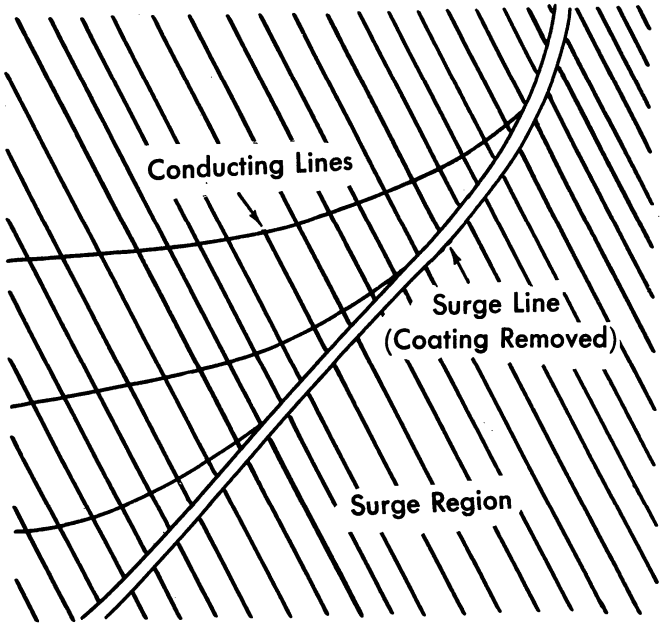

a. Earlier Method

FIG. 3a METHOD OF REPRESENTING THE SURGE LINE

plastic electrical tape, as shown in Figure 3b. This displaced the end effects well into the surge region and gave very good interpolation along the surge line itself. When the probe on the map reader touched the surge line, it became insulated from the function-generating surface and produced a discontinuity in the computer's operation, thereby giving an indication of surge.

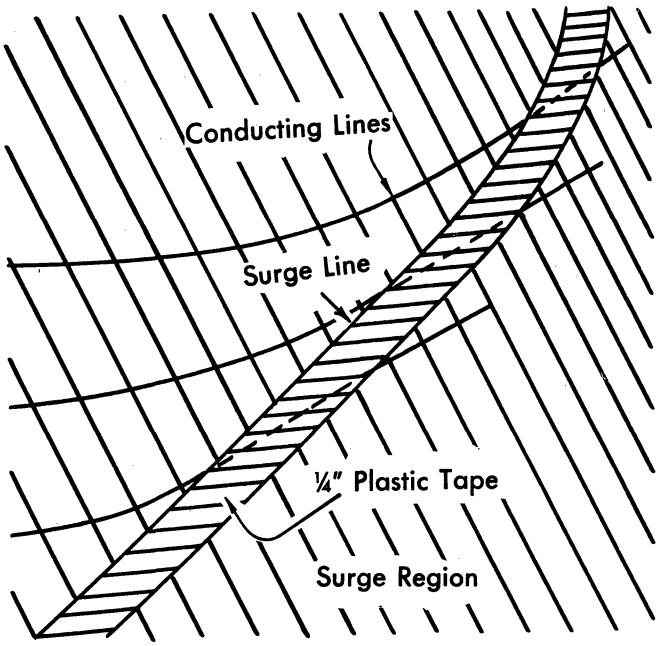

b. Later Method

FIG. 3b METHOD OF REPRESENTING THE SURGE LINE

2.4 Turbine Characteristics as Functions of Two Variables

For the first gas-turbine engine performance-computer ciruits, the turbine characteristics were assumed to be independent of rotor speed. For engines more recently simulated, however, the turbine characteristics were considered as functions of both pressure ratio and rotor speed. Thus, for simulating the turbine, the computer required two map readers, one giving corrected enthalpy drop as a function of pressure ratio and rotor speed, and the other giving corrected air-weight flow as a function of pressure ratio and rotor speed. The circuitry involving these functions in the turbine computer is shown in Figure 4. Note that the pressure ratio is obtained implicitly just as it was for the simpler engine as described on page 25 of Reference 1. The input quantities, shown at the left in Figure 4, are all obtained from other parts of the computer.

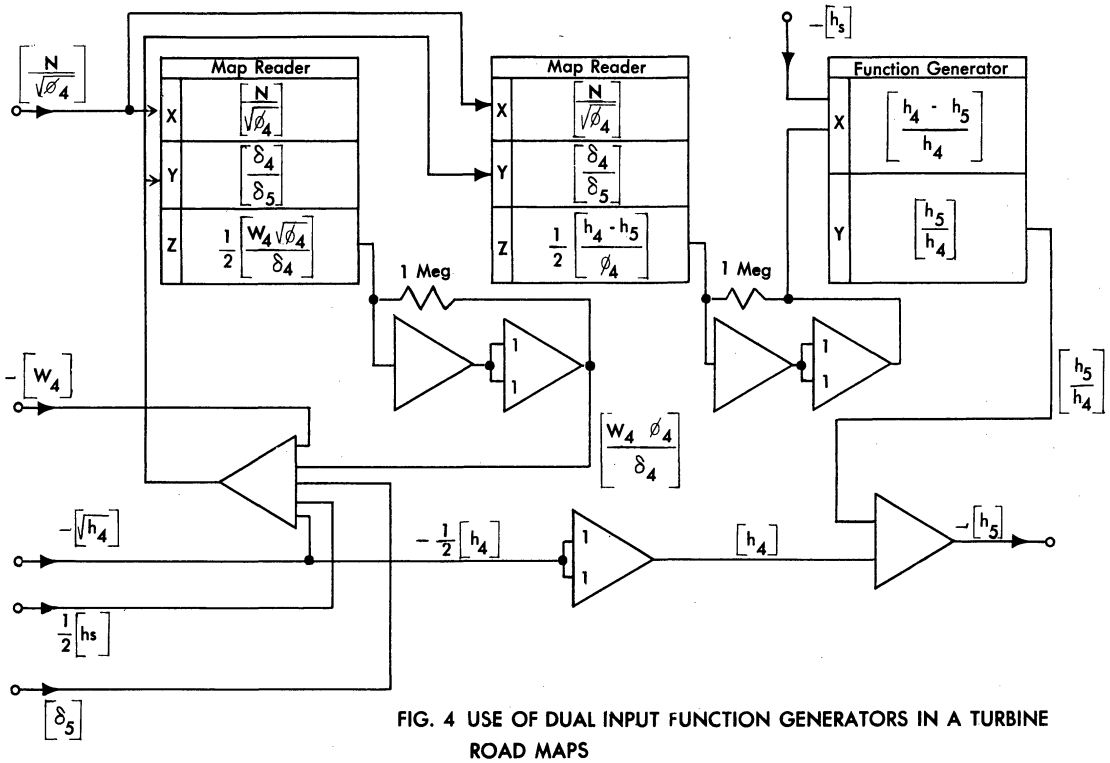

FIG. 4 USE OF DUAL INPUT FUNCTION GENERATORS IN A TURBINE ROAD MAPS

2.5 Variable Interstage Bleed in the Compressor

The problem of simulating variable interstage bleed is quite difficult, since bleed at an intermediate stage of the compressor affects the entire compressor map. It would be possible, of course, to have two compressor simulators, one for the stages of the compressor which precede the bleed point, and the other for the stages following bleed. This would require a considerable amount of additional equipment, however.

For one single spool engine which was simulated by the computer, the bleed was programmed as a function of rotor speed, and the compressor maps were altered to compensate for this. The compressor maps were plotted in terms of corrected air-weight flow at the compressor exit, with the programmed bleed in effect. The additional power required by the compressor to compress the bleed air was computed in a separate circuit as shown in Figure 5. The product of corrected bleed air-weight flow and corrected enthalpy rise for the bleed air,

$$\left(\frac{W_{BL}\sqrt{\theta_2}}{\delta_2}\right)\left(\frac{\Delta h}{\theta_2}\right) \text{ or } \left(\frac{W\,\Delta h}{\delta_2\sqrt{\theta_2}}\right),$$

which represented in corrected form the power required to compress the bleed air in the first stages of the compressor, was produced by the first function generator (Fig. 5) as a function of corrected rpm. The output of the function generator was then changed to $\left[\frac{\text{bleed power}}{N^2}\right]$ by adding logarithms of the necessary cancelling factors, in the amplifier A, and the result was changed to antilogarithmic form in the second function generator to permit it to be added to the compressor power in the rotor dynamics computer as a correcting term.

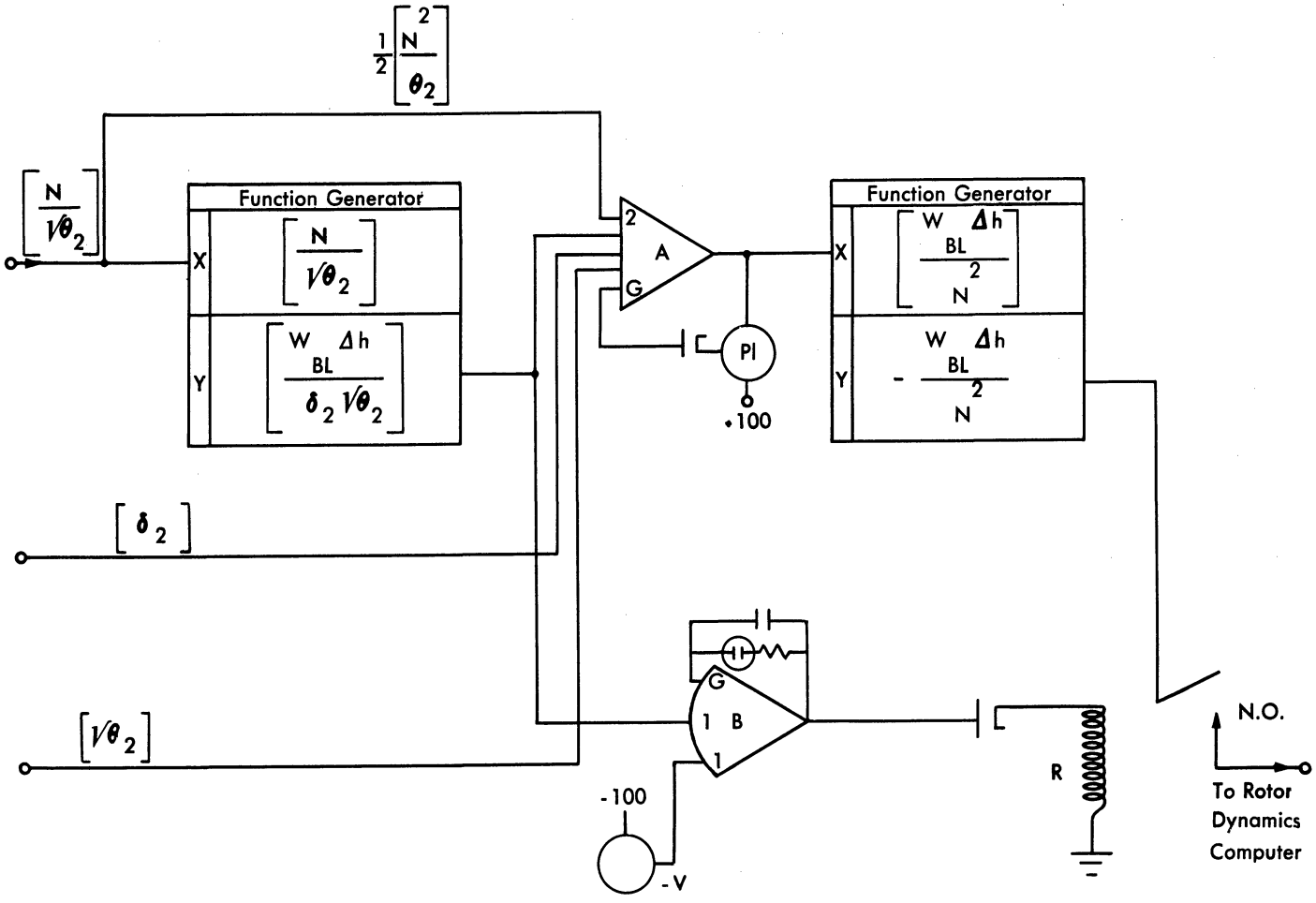

FIG. 5 CIRCUIT FOR COMPUTING POWER FOR COMPRESSING BLEED AIR

The relay R, whose coil is energized by the high-gain amplifier B through a diode, opens when the quantity $-\left[\frac{W_{BL}\,\Delta h}{\delta_2\sqrt{\theta_2}}\right]$ reaches a value corresponding to very low bleed power, and disconnects the circuit from the rotor dynamics computer. This relay is necessary to reduce the bleed power to zero, since zero cannot be represented logarithmically.

2.6 Improved Representation of Combustor Characteristics

In the earlier engine performance computers described in References 1 and 2, the enthalpy rise in the combustor was assumed to be a function only of fuel to air ratio. For one of the engines more recently simulated, the enthalpy rise was obtained as a function of both the fuel to air ratio and the combustor inlet enthalpy. The combustor enthalpy rise was produced by a dual-input function generator, with the logarithm of combustor efficiency times fuel/air ratio, $\eta b \frac{F}{A}$, on one input axis, and the logarithm of combustor inlet enthalpy h_3, on the other input axis.

A sketch of the plot is shown in Figure 6. Since the lines are nearly straight and evenly spaced, the function could have been approximated fairly accurately. In the example of Figure 6, it is apparent that:

$$\left[\Delta h\right] \approx K_1 + K_2\left[\eta_b \frac{F}{A}\right] - K_3\left[h_3\right] \qquad (1)$$

where K_1, K_2, and K_3 are constants chosen to make the approximation fit the curves.

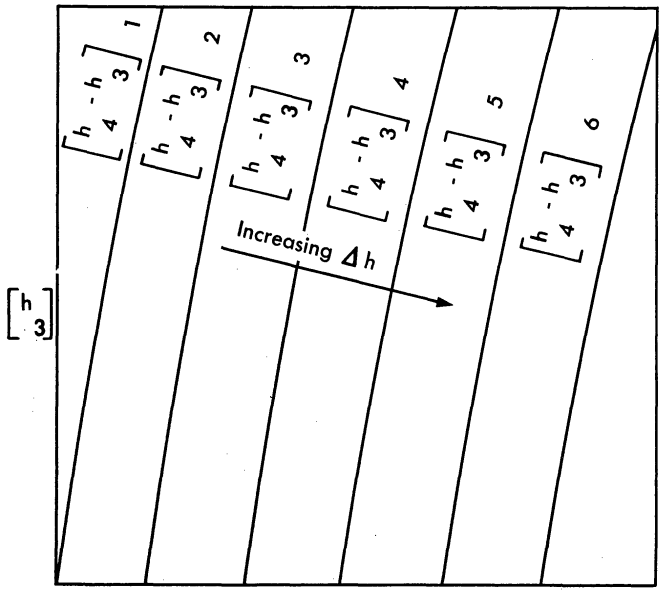

FIG. 6 ENTHALPY RISE IN A COMBUSTOR AS A FUNCTION OF $\left[\eta_b \frac{F}{A}\right]$ and $\left[h_3\right]$

A suitable computer "road map" for simulating the combustor characteristics in this manner is shown in Figure 7. Although it is an approximation to the actual two-variable function of Figure 6, it is still better than the approximation previously used, since it compensates for variations in the combustor inlet enthalpy.

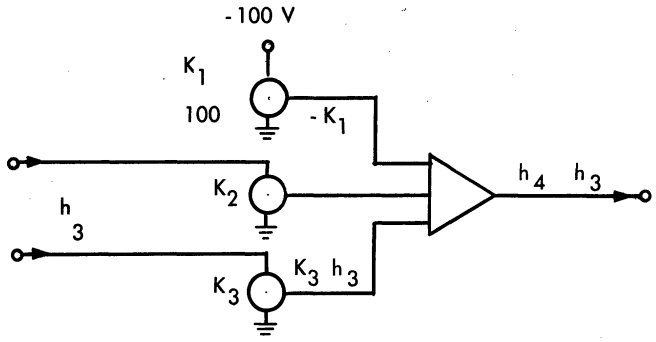

$$\left[h^4 - h^3\right] \approx K_1 + K_2\left[\eta_b \frac{F}{A}\right] - K_3\left[h_3\right]$$

FIG. 7 CIRCUIT FOR GENERATING $\left[h_4 - h_3\right]$ AS A FUNCTION OF $\left[\eta_b \frac{F}{A}\right]$ AND $\left[h_3\right]$

METHODS OF OPERATING THE PERFORMANCE COMPUTER

The purpose of this section is to describe the operating techniques which were employed to obtain various types of data from the computer. Although the methods were used with a twin-spool engine, most of them are also applicable to a single-spool engine. These methods are not especially recommended as the best, but instead they are presented as various techniques which have been used successfully for obtaining the desired data.

3.1 Data Conversion and Processing

In most cases when data were taken, the various d-c analog voltages from the computer were proportional in value to the logarithms of the various physical quantities which they represented. In other words, if X were some physical parameter used to describe operating conditions of the engine, such as temperature or pressure at a particular station, and if its analog computer voltage were V, then V was related to X by this equation:

$$V = C_1 \log C_2 X, \qquad (2)$$

where C_1 and C_2 were chosen for optimum scaling.

Logarithmic representation of variables gives improved accuracy and facilitates geometric operations such as multiplying, dividing, and raising to powers, but it has one outstanding disadvantage in that considerable time and effort and required to convert the computer voltages to the engine variables which they represent. This becomes especially troublesome in the process of trouble-shooting the computer.

This difficulty was overcome by plotting V versus X for Equation 2 on specially-constructed semi-logarithmic graph paper. If the plot is made on paper where the "V" scale is linear and the "X" scale is logarithmic, the result is a straight line which can be easily located by computing and plotting two of its points.

A separate conversion graph was made for each engine variable of interest. Then, the conversion from analog voltage to the corresponding value of the variable could be made quickly and easily be referring to the appropriate conversion graph.

In order to keep the conversion graph reasonably accurate, the logarithmic scale of the paper was constructed to cover one decade only. If the variations in an engine parameter covered two decades, two separate lines on the conversion chart were necessary. The conversion charts used were not accurate enough for some of the final data reduction, but this could have been remedied by using larger graphs and more accurate plots.

3.2 Determination of Engine Sensitivity to Changes in Control Parameters

Knowledge of the sensitivities of the engine's pressures, temperatures, and accelerations to changes in each of the control parameters (exhaust nozzle area, fuel flow, engine inlet conditions, and rotor speeds) is of considerable aid in designing an engine control system. Also, full knowledge of these sensitivities permits the design of a simple engine simulator, whose operation is linearized about some particular point. Each sensitivity is actually a partial derivative, showing the ratio of change of the dependent variable to the corresponding change in some independent or control variable, with all other independent variables held constant. If $(X_1 X_2 \ldots X_n)$ represent the independent variables, and Y a dependent variable, then for simultaneous small changes in the independent variables, the corresponding change in the dependent variable is given by

$$\Delta Y \cong \sum_{i=1}^{n} \frac{\partial Y}{\partial X_i} \Delta X_i \quad . \qquad (3)$$

Obtaining an equation similar to this for each of the important dependent variables, and having each partial derivative specified as a function of one or two dependent or independent variables gives all of the information needed to make a simple engine simulator.

The actual data obtained from the computer would be more correctly called increment ratios instead of partial derivatives. It was obtained from the computer as follows: A steady-state point for a given flight condition was simulated. The rotor speeds (or speed) were held constant, the independent variable whose effects were to be investigated was changed by a slight amount, and its change as well as the change in the dependent variable were recorded. The increment ratio was computed from the equation

$$\frac{\Delta Y}{\Delta X_i} = \frac{\text{(steady-state value of Y) - (value of Y after change)}}{\text{(steady-state value of } X_i\text{) - (value of } X_i \text{ after change)}} .$$

A digital voltmeter was used to read the initial and final values of each analog voltage and, while the change in $[X_i]$ was being made, a servo-driven $[X\text{-}Y]$ plotter was connected to plot $[Y]$ vs. $[X_i]$ in order to determine that the change occurred along an approximately linear region of $[Y]$ vs. $[X_i]$.

3.3 Variations in Engine Component Characteristics

Because of production variations in the manufacture of engine components, the operating characteristics of actual engines can show considerable differences from one engine to the next. For the twin-spool engine, a study was made to determine the effects on engine performance of slight changes in compressor characteristics and turbine characteristics. The effects were determined by first operating the computer with the standard compressor and turbine maps, and then introducing variations in compressor and turbine efficiencies and compressor air weight flow, while the computer was in operation. Since the variables were represented logarithmically, the changes were accomplished by simple adding slight fixed positive or negative voltages to the appropriate output voltages from the computer map readers. For example, if it was desired to decrease the air weight flow output of a compressor by 3 per cent for the same rotor speed and pressure ratio, it was necessary only to add a suitably-scaled fixed voltage representing log 0.97 to the voltage representing log $\frac{W\sqrt{\theta}}{\delta}$ obtained from

the appropriate compressor map, and use the sum of these two voltages (representing log $0.97\ \frac{W\sqrt{\theta}}{\delta}$) instead of the log $\frac{W\sqrt{\theta}}{\delta}$ voltage for other parts of the computer. A 3 per cent increase in air weight flow was accomplished by adding a voltage representing log 1.03 to the voltage representing log $\frac{W\sqrt{\theta}}{\delta}$. Efficiency changes were made by adding appropriate voltages to the outputs of those compressor and turbine maps containing enthalpy change as the dependent variable.

Comparison of engine operating data obtained before these changes with that obtained after the changes had been made immediately showed the effects of the changes. The changes were introduced separately, and in various combinations.

3.4 Use of Digital Voltmeter for Obtaining Steady-State Data

Much of the data were taken from the computer under steady-state conditions. For each operating point, the values of a large number of dependent variables were to be read. This process was accelerated by using a digital voltmeter as a read-out device, and connecting each variable to be read to a separate contact on a multiposition selector switch whose arm was connected to the digital voltmeter input.

A further modification of this read-out system consisted of substituting a stepping switch for the selector switch and connecting the digital voltmeter to a digital printing device (in this case a Clary adder whose keys were equipped with solenoids). This modification permitted each of the variables for a given steady-state condition of the computer to be read out and printed on the adding machine tape. Figure 8 is a block diagram of this latter arrangement. Unfortunately, it was not completed before technical work on the last project was halted, but it is expected to prove quite useful for future work.

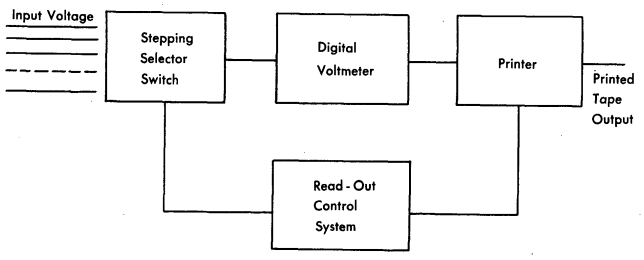

FIG. 8 BLOCK DIAGRAM OF AUTOMATIC DIGITAL READ-OUT SYSTEM FOR AN ANALOG COMPUTER

3.5 Surge Behavior of a Twin-Spool Engine

Determination of surge conditions for a single-spool engine is relatively simple, and the procedure has been described in Reference 1. For a twin-spool engine, however, a larger number of variables is involved and a systematic definition of surge conditions is more difficult. The surge behavior of the twin-spool engine was investigated by considering two fundamentally different methods of obtaining the surge conditions. For one mode, the surge characteristics of the engine were obtained as a function of fuel flow, and the simulation was performed in the following manner: After a steady-state operating point of interest (representing a preassigned flight condition, and power setting of fuel-flow and nozzle throat area) had been obtained on the computer, the rotor speeds were held constant and the fuel flow was increased until the surge line of one of the compressors was reached, or the design limit on T_4 had been obtained. Pertinent engine data for this condition were then recorded. This operation was then repeated for the same flight conditions but at different power levels in order to obtain surge on each compressor.

The second surge mode investigated was intended to show the effects of the high-pressure rotor speed on surge. First, a steady-state operating condition was set into the computer as for the previous method, and then the speed of the high-pressure rotor was adjusted (while holding the low-pressure rotor speed constant) until a surge condition was obtained for one of the compressors. Here too, a number of various power levels was investigated for each flight condition in order that surge on each compressor as well as the design limit on T_4 could be achieved.

3.6 Exploration of Engine Flight Spectrum Limits

In accordance with performance specifications, an engine must operate at rated power over a certain range of altitude, mach number, and ambient temperature. If planes representing the limits of each of these ranges are plotted on a three-dimensional Cartesian coordinate system, with one axis corresponding to altitude, another to mach number, and the third to ambient temperature, the volume enclosed by these planes contains all possible combinations of altitude, mach number, and ambient temperature which lie within the specified limits of the engine's operation and constitutes the engine's flight spectrum. This is illustrated by Figure 9.

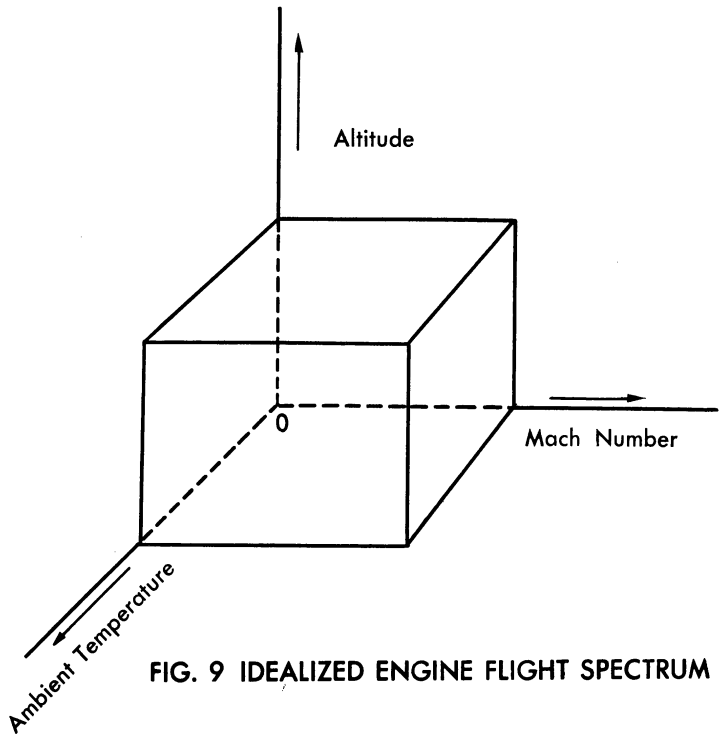

FIG. 9 IDEALIZED ENGINE FLIGHT SPECTRUM

Ideally, the engine should be able to operate at any point on the surface of this figure, but in practice the engine is prevented from operating in all sections of this spectrum by various limiting conditions. For example, the mach number must be limited at low altitudes in order to prevent excessive pressures after the compressor which may cause structural failure of the engine. For the lower altitudes, the maximum mach number is limited by the maximum difference between the ambient pressure and that at the compressor exit which may be developed without exceeding the engine's structural limitations. Other limiting factors are the maximum permissible turbine inlet temperature, T4, and the burning limits within the combustor. Thus, the actual flight spectrum will depart from that shown in Figure 9.

If the inlet conditions are properly adjusted, the computer may be made to operate at any desired combination of altitude, mach number, and ambient temperature; and those combinations which cause the compressor exit pressure or the turbine inlet temperature to exceed their specified limits may be easily determined. In this manner, the engine's "flight spectrum" may be readily explored in order not only to determine the actual limits of engine operation, but also to determine the engine's behavior at all other points. The amount of operation necessary may be reduced considerably by exploration of the edges of the flight spectrum, since these represent its boundaries, and, therefore, the extremes in operating conditions.

The operating ranges of the compressor maps should be extended to permit operation about 25 per cent above the normal sea-level static operating point in order to insure that the probes will not go off the map when flight spectrum exploration is attempted.

4

SIMULATION OF ENGINE CONTROLS

Methods of programming the maximum fuel-flow as a function of rotor speed for the single rotor engine are described in Reference 1, and a circuit to represent the dynamics of a propeller pitch control is described in Reference 2. For the twin-spool engine, no scheduling controls were simulated, but the dynamics of the steady-state control were simulated, on a separate computer, which was then connected to the engine computer. The control simulation was straightforward, using proportional instead of logarithmic representation of variables. Since the details are of a proprietary nature, no description of the control simulator is included in this report. A relatively simple but accurate method of determining the frequency response of the simulated control was discovered, however, and this method is described in the following paragraphs. A description of a method of simulating mechanical backlash is also included.

4.1 Measurement of Frequency Response

The output of a linear network which is being driven by a constant amplitude sinusoidal input signal of constant frequency is a sinusoid of the same frequency as the input but having a different amplitude and phase angle. Figure 10 is a block diagram showing an electrical network being driven by a sinusoidal voltage generator. G(jω) is the frequency-response function of this network.

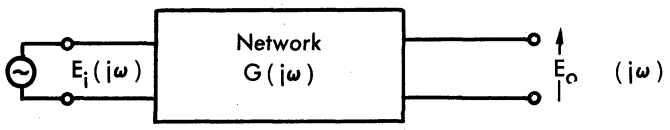

FIG. 10

NETWORK DRIVEN BY A SINUSOIDAL VOLTAGE

E_i and E_o are the r.m.s. values of the input and the output signals, respectively, and $\theta(\omega)$ is the angle by which the phase of the output sinusoid leads that of the input. In polar coordinates, this may be expressed as

$$\left| G(j\omega) \right| = \frac{E_o}{E_i} = \rho \qquad (5a)$$

$$\text{Arg.}\,[G(j\omega)] = \theta \qquad (5b)$$

or, in rectangular coordinates

$$G(j\omega) = \frac{E_o}{E_i}\cos\theta + j\,\frac{E_o}{E_i}\sin\theta = x + jy \ . \qquad (6)$$

The analytical expression for G(jω) is obtained by first deriving the transfer function, G(s), and then substituting jω for s. The resulting expression may be evaluated easily for any specific ω to provide a check against results obtained when the response to a sinusoid with the same ω is measured. These results may be expressed in terms of an amplitude ratio and a phase angle, as in Equations 5a and 5b, or in terms of real and imaginary components, as in Equation 6.

Two methods of measuring the frequency response of the controls were tested. The first method involved direct measurement of amplitude and phase angle. A sinusoidal voltage was generated by a computer circuit which solved the equation $\ddot{X} + \omega^2 X = 0$, and this voltage, suitably scaled in magnitude and frequency, was applied as the driving signal to the computer circuit whose response was to be measured. The input voltage, E_i, and the output voltage, E_o, were connected into adjacent channels on a four-channel recorder. The ratio of amplitudes of the recorded waves gave $\frac{E_o}{E_i}$, and the temporal displacement of the output waveform with respect to the input waveform on the recorder paper gave the phase angle θ.

This method of measurement was found to be unsatisfactory since, even if possible errors in recorder calibration were neglected, the average error in amplitude measurement was over 5 per cent, and the error in phase-angle measurement was on the order of 10^o.

In order to remedy these difficulties, a circuit for accurately measuring the rectangular-coordinate components of G(jω) was devised. Equation 6 may be rewritten as

$$G(j\omega) = \frac{E_o\cos\theta + j\,E_o\sin\theta}{E_i} \ . \qquad (7)$$

The term, $E_o \cos\theta$, which constitutes the real part of the numerator, is the component of output voltage which is in phase with E_i. The term, $j\,E_o \sin\theta$, represents the component of output voltage which is 90^o ahead of E_i.

Figure 11 shows the circuit used for measuring frequency response. The two integrators, A and C, and the inverting amplifier, B, make up a circuit for generating the driving sinusoid (K sin ω t). The circuit generates (K sin ω t)by solving the equation, $\ddot{X} + \omega^2 X = 0$, with the correct initial conditions. Another way of regarding this circuit's operation is to assume that the output of integrator C is -(K cos ωt). This assumption is true for t = 0, if the initial condition potentiometer, P1, is set to give -K as the output of integrator C before the circuit starts to operate. Then, when the circuit is in operation, potentiometer 3 multiplies the output of integrator C by ω to give -(K ω cos ωt) as an input to integrator A. Integrator A integrates this input with respect to t and inverts the result to give (K sin ω t) as an output. The quantity K sin ω t is inverted in sign by amplifier B to give -(K sin W t). Potentiometer 2 multiplies this quantity by ω to give -(K ω sin ω t) as an input to integrator C. Integration of -(K ω sin ω t) by integrator C gives -(K cos ω t) at C's output, thus validating the original assumption.

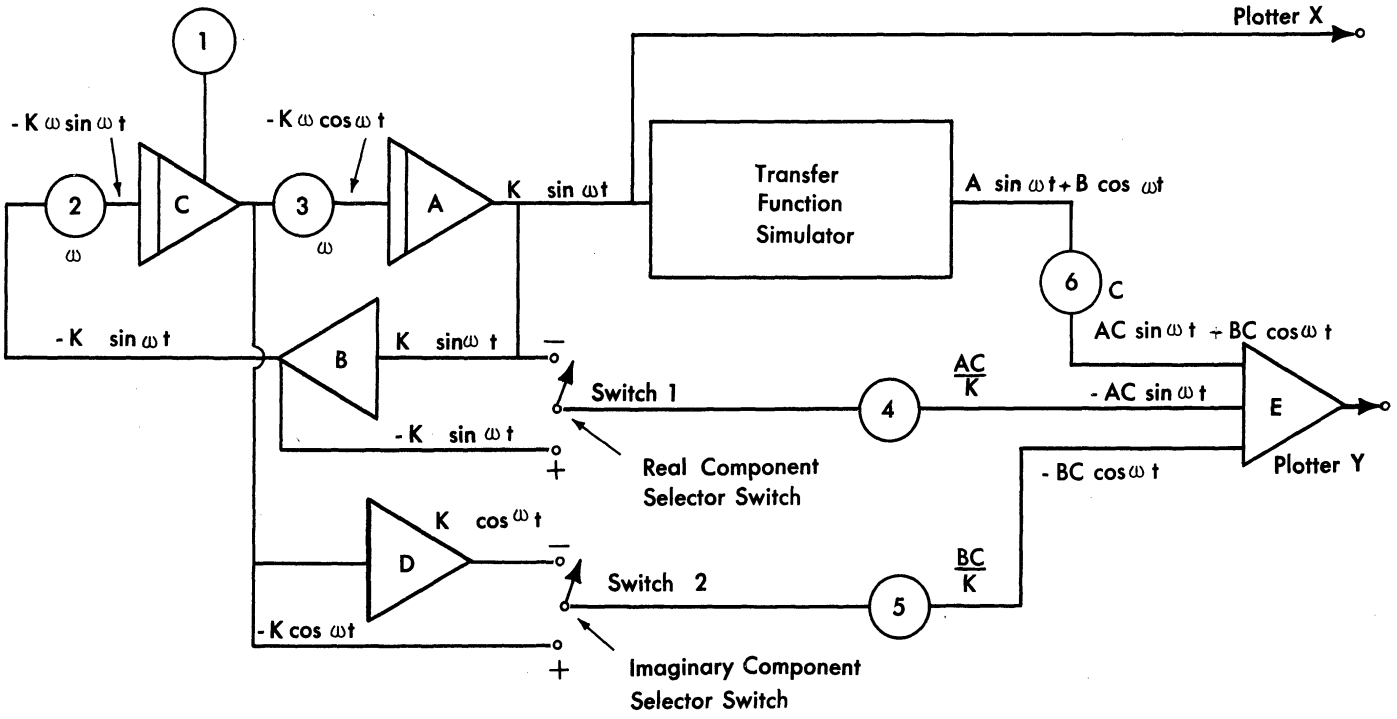

FIG. 11 CIRCUIT FOR MEASURING FREQUENCY RESPONSE

The output of integrator A provides the forcing function for the input of the transfer function simulator circuit. When the circuit's input is (K sin ω t), its steady-state output will be of the form (A sin ωt + B cos ωt) if the circuit is composed entirely of linear elements.

The term A sin ω t) represents the component of the output which is in phase with the input, so the ratio, $\frac{A}{K}$, is equal to the real part of the transfer function, G(jω). The term (B cos ωt) in the output represents the component of the output which leads the input by 90°, and thus the ratio, $\frac{B}{K}$, represents the imaginary component of G(j ω), corresponding to $j\frac{E_o}{E_i}\sin\theta$ in Equation 6.

Potentiometer C multiplies the output of the transfer function circuit by a constant "C" to give (AC sin ω t + BC cos ω t) as an input to amplifier E. A second input to amplifier E is -(AC sin ω t), obtained by choosing either (K sin ω t) or -(K sin ω t) at switch 1, and passing the result through potentiometer 4, which is set to $\frac{AC}{K}$. The third input to amplifier E is -(BC cos ω t), obtained by choosing either (K cos ω t) or -(K cos ω t) at switch 2, and passing the result through potentiometer 5 which is set to $\frac{BC}{K}$. Obviously, if potentiometers 4 and 5 and switches 1 and 2 are set correctly, the output of amplifier E will be zero. The circuit is operated by setting switches 1 and 2 and adjusting potentiometers 4 and 5 to give zero output for amplifier E. Then, since $\frac{A}{K}$ = Re(G(j ω)), the setting of potentiometer 4 is C(ReG(j ω)). Similarly, the setting of potentiometer 5 is C(ImG(j ω)). If G(j ω) has a positive real component, (A sin ω t) will be positive, and switch 1 must be set to the plus position to feed -(K sin ω t) into potentiometer 4, in order that this potentiometer's output may cancel the (A sin ω t) term coming from the transfer function simulator. If G(j ω) has a negative real component, then +(A sin ω t) must be obtained from potentiometer 4 to cancel this component, and switch 1 must be set to the minus position.

Switch 2 acts in a similar manner to give the correct polarity to cancel out either a positive or negative imaginary component in the output of the transfer function simulator. If |G| is not greater than unity, potentiometer C may be by-passed, and the settings of potentiometers 4 and 5 will give the real and imaginary components of G(j ω) directly.

The adjustment of potentiometers 4 and 5 is facilitated by using a servo-driven X-Y plotter as the null indicator on the output of amplifier E. With the plotter's Y-input connected to amplifier E and its X-input connected to the signal driving the transfer

function simulator, it traces a figure indicating which of the components (sine or cosine) is still present in still present in amplifier E's output. If the output of amplifier E remains at zero, thus indicating proper adjustment of potentiometers 1 and 2, the plotter produces a horizontal straight line. If the plotter traces a diagonal straight line, the sine component is still present in amplifier E's output, thus indicating that potentiometer 4 is adjusted incorrectly. If the plotter produces an ellipse, with one of the axes of the ellipse horizontal, the cosine component is still present in amplifier E's output, and potentiometer 5 requires further adjustment. If the figure traced by the plotter is an ellipse with axes not parallel to the plotter's coordinate system, both potentiometers 4 and 5 need to be readjusted.

This circuit permits measurement of the real and imaginary parts of $G(j\omega)$ to within about 0.05 per cent if a bridge-type potentiometer checker is used for reading the settings of potentiometers 4 and 5 after a null has been obtained. The nulling error may be considered negligible.

If the transfer-function simulator contains nonlinearities, such as dead space and limiting, its output will no longer be exactly sinusoidal, but it will contain various harmonics of the driving signal. It is feasible, however, by using the X-Y plotter as a null indicator, to cancel out the fundamental in the output, and thus obtain points on the "describing function" for the network. In this case it is more difficult to obtain a null, since the harmonics tend to mask the presence of the fundamental.

4.2 Simulation of Mechanical Backlash

Simulation of one of the controls involved introducing mechanical backlash or hysteresis into the system. Both position and velocity information were to be transmitted through the linkage which had the backlash. The circuit for accomplishing this was somewhat different from those usually published in the literature, and thus it is included in this report.

Figure 12a illustrates a system with mechanical backlash. It consists of two sliding bars whose ends are loosely coupled. If bar 1 is pushed to the right, x_1 increases, but there is no motion of bar 2 (change of x_2) until the gap in the coupling between the two bars is closed. Then, as long as x_1 continues to increase, x_2 increases at the same rate as x_1. If bar 1 is now moved to the left, x_1 decreases while x_2 remains constant until the gap in the coupling is closed, and then x_2 decreases at the same rate as x_1. If the motion of bar 1 is reversed at any time when bar 1 is driving bar 2, bar 2 will remain stationary until bar 1 has been moved by an amount equal to the dead space in the coupling. If bar 1 oscillates back and forth by an amount equal to, or less than, the dead space in the coupling, bar 2 does not move.

The computer circuit for simulating this effect is shown in Figure 12b. The input to the system is $\dot{x}_1$, and the outputs are x_2 and $\dot{x}_2$. The quantity $\dot{x}_1$ drives integrator A to produce $-x_1$ as an input to amplifier B. The relative velocity between the two bars $(\dot{x}_1 - \dot{x}_2)$ is equal to $\dot{x}_1$ as long as bar 1 is not touching bar 2, since $\dot{x}_2$ is zero under these conditions. As soon as bar 1 has made contact with bar 2, the two bars have the same velocity, and the quantity, $(\dot{x}_1 - \dot{x}_2)$, becomes zero. The quantity $(x_1 - x_2)$ is limited to the amount of free motion existing between bar 1 and bar 2.

The circuit may be more easily explained by first considering its action with the limiting circuits, containing the diodes and potentiometers, removed. This condition corresponds to no coupling (or an unlimited amount of backlash) between bars 1 and 2 in Figure 12a. Any $\dot{x}_1$ voltage existing at the input of the circuit causes the output voltage of integrator A to move in one direction and output voltage of integrator F to move in the other direction (because of the inversion of the $\dot{x}_1$ voltage in passing through amplifiers C, D, and E). The output of amplifier B remains constant because one of its input voltages is increasing while the other is decreasing at the same rate. Thus, x_1 varies while x_2 remains constant.

If limiting circuits are added, the quantity, $(x_1 - x_2)$, is limited at the output of integrator F to the amount of play in the coupling between bars 1 and 2. When this limit is reached, the output of integrator F remains constant, while the output of integrator A continues to change. Thus, the output of amplifier B, or x_2, starts to change at the same rate. If the sign of $\dot{x}_1$ is then reversed, the outputs of integrators A and F will both change and x_2 will remain constant until the output of integrator F reaches its other limit. Then, the quantity $(x_1 - x_2)$ will again remain fixed and the output of amplifier B will start to change.

The limiting is accomplished by feedback circuits consisting of potentiometers and diodes as shown. The setting of potentiometer P1 determines the negative limit of $(x_1 - x_2)$, while the setting of potentiometer P2 determines the positive limit. If the output of integrator F is zero, the arm of poten-

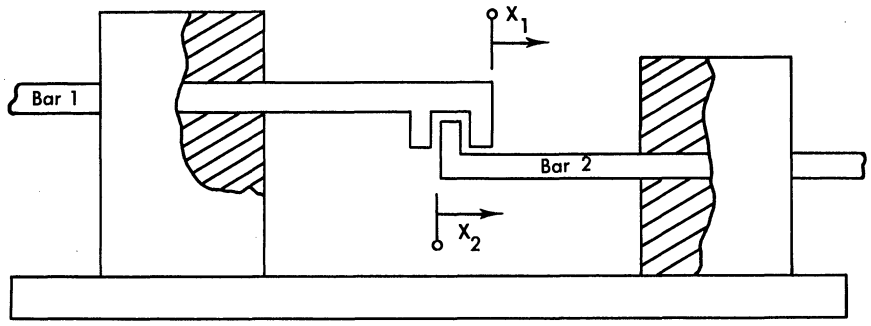

a. Example of Mechanical Backlash

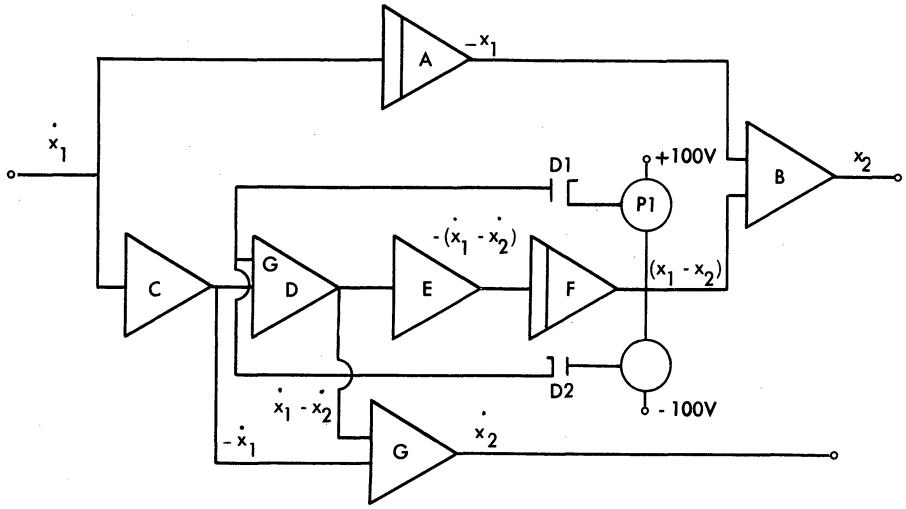

b. Computer Circuit for Simulating Mechanical Backlash

FIG. 12 SIMULATING MECHANICAL BACKLASH

tiometer P1 is positive with respect to ground, and the arm of P2 is negative, so neither diode D1 nor D2 is conducting. Now, assume that some positive value of $\dot{x}_1$ is impressed on the input of the circuit. The output voltage of amplifier C will be negative, that of amplifier D will be positive, and that of amplifier E will be negative. This negative input voltage to integrator F will cause the output voltage of this integrator to change in a positive direction. This change causes the arms of both potentiometers, P1 and P2, to become more positive. When the arm of P2 becomes positive with respect to ground, diode D2 conducts, and a positive current is carried back to the input grid of amplifier D. If this positive input current exceeds the negative current coming from amplifier C, the output of D becomes negative, that of E becomes positive, and the output of integrator F begins to move in a negative direction, thus tending to decrease the current fed back through diode D2. If, on the other hand, the feedback curcent is less than the current entering D from amplifier C's output, the output of integrator F will become more positive and will cause this current to increase. The circuit tends toward an equilibrium point where the output of integrator F is not changing and where, consequently, the output of amplifier D is zero.

Potentiometer P1 and diode D1 limit the negative excursions of integrator F's output in the same manner as P2 and D2 limit the positive excursions.

Amplifier G sums the outputs of amplifiers C and D to give $\dot{x}_2$. When neither of the limiting circuits is in operation, the output of D is the negative of the output of C, thus causing the output of amplifier G to be zero. Then, for the conditions where bar 1 has made contact with bar 2 in Figure 12a, $\dot{x}_2$ is equal to $\dot{x}_1$. This condition corresponds to the point where limiting occurs in the output of integrator F in Figure 12b, and, since under these conditions the output of amplifier D is zero, the output of amplifier G is the same as the $\dot{x}_1$ entering the system.

BIBLIOGRAPHY

1. Larrowe, V. L., Spencer, M. M., and Tribus, M. L. A Dynamic Performance Computer for Gas Turbine Engines. The University of Michigan, Engineering Research Institute. Contract No. AF 33(616)-2074. Phase I Final Report, WADC TR 54-577. Part I, December 1953.

2. Larrowe, V. L. and Spencer, M. M. A Dynamic Performance Computer for Gas Turbine Engines. The University of Michigan, Engineering Reasearch Institute. Contract No. AF 33(616)-2074. Phase II Final Report, WADC TR 54-577. Part II, August 1955.

3. Larrowe, V. L. and Spencer, M. M. "Use of Semi-Conducting Surfaces in Analog Function Generation." Proceedings of the National Simulation Conference, Dallas, Texas. January 1956. pp. 33.1-33.6.